DTU Library

Structural characteristics of low-density environments in liquid water

Muthachikavil, Aswin V.; Kontogeorgis, Georgios M.; Liang, Xiaodong; Lei, Qun; Peng, Baoliang

[Link back to DTU Orbit](#)

Structural Characteristics of Low Density Environments in Liquid Water

Aswin V. Muthachikavil, Georgios M. Kontogeorgis, and Xiaodong Liang*

Center for Energy Resources Engineering, Department of Chemical and Biochemical Engineering,
Technical University of Denmark, Kgs. Lyngby 2800, Denmark

Qun Lei and Baoliang Peng†

Research Institute of Petroleum Exploration & Development (RIPED), PetroChina, Beijing, China
(Dated: March 2, 2022)

The existence of two structural forms in liquid water has been a point of discussion for a long time. A phase transition between these two forms of liquid water has been proposed based on evidence from molecular simulations, and experiments have also been very recently able to track the proposed transition of the low-density liquid (LDL) form to the high-density liquid form. We propose to use the average angle an oxygen atom makes with its neighbors to describe the structural environment of a water molecule. The distribution of this order parameter is observed to have two peaks, with one peak at ∼ 109.5°, corresponding to the internal angle of a regular tetrahedron, indicating tetrahedral arrangement. The other peak corresponds to an environment with a tighter arrangement of neighboring molecules. The distribution of O-O-O angles is decomposed into two skewed distributions to estimate the fractions of the two liquid forms in water. A good similarity is observed between the temperature and pressure trends of fractions of locally favoured tetrahedral structure (LFTS) form estimated using the new order parameter and the reports in the literature, over a range of temperatures and pressures. We also compare the structural environments indicated by different order parameters and find that the order parameter proposed in this work captures the structure of first solvation shell of LFTS accurately.

I. INTRODUCTION

Water's anomalous properties are important to many fields of human interests, placing it at the center of human curiosity for a long time. The two-state theory proposes that water's anomalies are exhibited in a funnel shaped region on the phase diagram where there are fluctuations between two structural forms [1–6]. This region is hence often described as the funnel of life [5]. Even though the idea of modelling water as two liquid forms is quite old [7, 8], it gained more attention in the recent times because of its potential to explain the anomalies of water at ambient and super-cooled conditions [9–16]. Different authors have contested and debated the two-state model for water, including Tanaka [1, 3, 4], Anisimov [13, 17–19], Stanley [16, 20–22], Limmer and Chandler [23–25], and Nilsson and Pettersson [5, 26–30], to name a few.

The two structural forms of liquid water have been linked to the two forms of amorphous ice - the high density and the low density amorphous ice (HDA and LDA, respectively), which have been observed to have a first-order-like phase transition between them [31]. Transition temperatures between the glassy solids HDA and LDA to high density liquid (HDL) and low density liquid (LDL) respectively have also been reported in the literature [32, 33]. Even though these experimental works pointed to the existence of two structural environments in water, the phase transition between LDL and HDL has been observed only recently. Nilsson et al. were able to follow the transition of LDL to HDL at deeply supercooled temperature of -163 °C using a combination of experimental techniques [28, 30]. This work provided experimental evidence to the existence of the two hypothesised forms of liquid water and the transition between the two.

It is of interest to note that the first evidence of the liquid-liquid critical point in water was from molecular simulations. In a seminal work, Poole et al. used molecular simulations of the ST2 water model, which suggested that the anomalous behaviour of water in the supercooled regime could be the result of the presence of a second (liquid-liquid) critical point [20]. The aim of this study was to test the extent to which molecular simulations would be able to cope with the 'Speedy limit conjecture' [34]. But their results suggested a different phase diagram with the existence of a liquid-liquid critical point (LLCP). These results were challenged by Chandler and Limmer [23], who argued that the observations which were attributed to a liquid-liquid transition were in fact associated with a liquid-crystal transition. The heated discussion [25, 35, 36] came to a conclusion only recently, when a conceptual error in the model of Chandler and Limmer was uncovered [37, 38]. Debenedetti et al. very recently explored the existence of second critical point using simulations [39] and observed significant fluctuations in density between two average values. They also estimated the critical points for the TIP4P/2005 and TIP4P/Ice water models, supporting the existence of the proposed LLCP at positive pressures for water.

After it was shown that the existence of LLCP cannot be excluded, the relevance of estimation of structure and

---

* xlia@kt.dtu.dk
† pengbl@petrochina.com.cn

properties using the two-state picture has grown. Many research groups have studied the two-state picture of water, not just in terms of exploring the LLCP and liquid-liquid phase transition (LLPT), but also validating and characterising the existence of two forms of liquids in different conditions including the ambient [14, 29, 40]. Different methods have been proposed to distinguish and study the two states of water in molecular simulations of different water models.

A notable effort in characterising the two structural forms of water was by Pettersson et al. [40], who reported the Local Structure Index (LSI) [41] using molecular simulations. The *inherent structure* [40, 42] showed a bi-modal distribution of LSI indicating two characteristic types of ordering in water. Tanaka et al. [14] used the TIP4P/2005 and TIP5P water models to look at the distribution of LDL and HDL in liquid water in a wide range of temperatures, using a structural descriptor [6]. They proposed that locally favoured structures are formed in a sea of 'normal liquid'. Shi and Tanaka have reported a comparative study on the structures described by some of the currently existing order parameters, using molecular simulations [43]. Structural heterogeneities in liquid water have also been studied in molecular simulations by characterizing density fluctuations with empty voids with diverse morphology [44]. These voids were characterized for the identification of low density patches using the concept of Voronoi S-Network [45, 46]. Very recently, Shi and Tanaka [47] showed that the bimodailty in the coordination number and the *structure factor* in molecular simulations of liquid water supports the two- state theory of water. They argued that presence of the first sharp diffraction peak is indicative of tetrahedral environments in water. Even though different parameters that quantify structuring of water molecules are able to show two distinct structures in water indicated by a bi-modal distributions of order parameters, they cannot distinctly demarcate the two structures because of the overlap in distributions. This is an indication of environments with mixed character [27]. The degree of heterogeneity and the boundaries of the fluctuating structures in water are still open questions.

In this work, we use the angles that oxygen atoms make with its nearest neighbors to characterize the tetrahedral environment of water. Even though the distributions of angles formed by oxygen atoms have been studied *a priori* for different purposes [48–57], it has not been utilized yet to estimate the fractions of the two structural forms in water, to the best of our knowledge. We demonstrate that the bi-modal distribution of the O-O-O angles may be decomposed to two Gaussian components corresponding to the two locally favoured structural forms in water. This is then used for estimating the fraction of locally favoured tetrahedral structures (LFTS) [58] in water (the term LDL is also often used in the literature by some authors [27, 59]) and studying the structural characteristics of the low density form of water.

Urbic and Dill [60] proposed a model of a 'cagey wa-

ter' assuming that liquid water has an underlying hexagonal ice structure, and the disordered liquid structure is a perturbation to the tetrahedral structure. They also demonstrated the ability of this model to calculate the properties of bulk water. We also show that this assumption of existence of tetrahedral structure of ice I_h is true in liquid water, by comparing the scatter of different order parameters in water and ice I_h. We also report the probabilities that any given water molecule belongs to a tetrahedral environment, provided we know the average angle it makes with its neighbors. To comment on the two structural forms of water, we also compare the structural environments indicated by other order parameters, with the tetrahedral environment indicated by the O-O-O angles.

II. METHODS

A. Molecular simulations

Molecular simulations were performed using the polarizable iAMOEBA water model [61], which reproduces properties like density, dielectric constant, self-diffusion coefficient and vapor-liquid equilibrium curve [59, 62–64]. In extensive review articles, the iAMOEBA model was found to perform excellent in comparison to many widely used water models in capturing the bulk, critical, vapor-liquid equilibria and thermodynamic properties of liquid water [62, 64]. NPT simulations were performed (with 2094 molecules), generating trajectories ranging from 10 ns to 100 ns, using OpenMM 7.5 [65]. Longer simulation lengths were used for analysis at lower temperatures. Time step integration was performed using Langevin leap-frog integrator [66], with a time step of 1 fs. Pressure coupling was done using Monte Carlo barostat [67, 68], with a coupling time of 2.5 ps. Simulation trajectory was written out at every 10 ps. The MDAnalysis library [69] was used to read the simulation trajectories, and compute the properties of interest from the trajectory.

B. Gaussian mixture decomposition

The first shell neighbors of a molecule are identified by a cut-off of 3.7 $\mathring{A}$ [41]. The distribution of the average angle formed by oxygen atoms with neighbors ($P(\theta)$) was observed to be decomposable to two skewed Gaussian distributions (see Fig. 1a) as shown in equation 1.

$$
\begin{aligned}
P(\theta) =& s * G_{skew}(\theta; \mu_s, \sigma_s, \alpha_s) \\
&+ (1 - s) * G_{skew}(\theta; \mu_\rho, \sigma_\rho, \alpha_\rho)
\end{aligned}
\tag{1}
$$

where s is the weight of the skewed Gaussian distribution corresponding to the s-form (tetrahedrally structured) and $1 - s$ is the fraction of ρ-form (non-tetrahedral

form). The individual skewed distributions [70] are given by equation 2.

$$G_{skew}(\theta; \mu, \sigma, \alpha) = \frac{1}{\sigma\sqrt{2\pi}} \exp\left(-\frac{\theta - \mu}{2\sigma^2}\right)$$
$$\times \left[1 + erf\left(\frac{\alpha(\theta - \mu)}{\sigma\sqrt{2}}\right)\right] \quad (2)$$

where μ, σ and α are parameters of the skewed Gaussian distribution, and $erf(x)$ is given by

$$erf(x) = \frac{2}{\sqrt{\pi}} \int_0^x e^{-t^2} dt \quad (3)$$

We estimate the parameters of equation 1 by minimising the square of deviation between distribution of θ estimated from simulations and the sum of the Gaussian components as calculated by equation 1.

III.   RESULTS AND DISCUSSIONS

A.   Estimating the fraction of LFTS

In a tetrahedral local environment in water, oxygen atoms form an angle of $\sim 109.5^o$ with all its neighbors. An oxygen atom makes $\binom{n}{2}$ angles with its n nearest neighbors. For example, a molecule having four neighbors can form $\binom{4}{2} = 6$ angles with its neighbors. Even though the tetrahedrality can be well captured by looking at distribution of all the $\binom{n}{2}$ angles (See section S1 in supplemental material [71] for a brief discussion), the *average angle* an oxygen atom makes with all its neighbors can be beneficial, defined as

$$\theta_{avg} = \frac{\sum_{i=1}^n \sum_{j=i+1}^n \theta_{ij}}{\binom{n}{2}} \quad (4)$$

where θ_{ij} is the angle a given oxygen atom makes with its ith and j^{th} neighbors. This assigns one single value of θ_{avg} to an oxygen atom. When an oxygen atom belongs to a tetrahedral environment, all the angles it makes with its neighbors lie around $\sim 109.5^o$, leading to an average not very different from the individual angles. However, in a non-tetrahedral environment, an oxygen atom is likely to form smaller angles (forming tighter orientations) with two or more of its neighbors. This would lead to a reduction in the average angle compared to that of a structured tetrahedral environment. Here, we would like to emphasize that the method of using O-O-O angles to characterise tetrahedral environments is based on the geometric structure of tetrahedra, and not on the underlying potential of the water model. Therefore, in principle the method described in this work would be transferable to any other water model which captures the structure and ordering in liquid water. To demonstrate this to the readers, we have added results from simulations of the

TIP4P/2005 water model (see section S2 of supplemental material [71] for details). Fig. 1b shows the distribution of *average angles* an oxygen atom forms with its neighbors.

The fraction of tetrahedral structural forms in water was estimated by the weights of individual Gaussian components (see Methods and section S3 in the supplemental material [71] for the discussion and the estimated values of the parameters of equation 1 at all the conditions reported in the study.), and is shown in Fig. 2a. The nature of the curves are in line with those predicted from molecular simulations [6, 59] and two-state thermodynamic models [13, 72]. The fraction of tetrahedral liquid form is observed to increase when the temperature is reduced, with a sharper change in a temperature range of 210-230 K. Another similar approach reported by Russo and Tanaka [6] utilized ζ parameter as a structural descriptor (see equation 1 in supplemental material [71]) to identify locally favored structures. A comparison of the LFTS fractions estimated using θ_{avg} and the values reported by Russo and Tanaka (using ζ) was done and a (qualitatively) similar temperature-trend was observed (See Fig. S3b and the associated text in the supplemental material [71] for details).

We also compared the fraction of LFTS molecules estimated by θ_{avg} with the fraction of tetrahedral environments indicated by hydrogen bond formation. In a recent work [73], we used Potential of Mean Force (PMF) landscapes to distinguish 'ice-like' hydrogen bonds in liquid water. Two molecules are defined to be hydrogen bonded if the oxygen-hydrogen (O–H) distance and the oxygen–hydrogen-oxygen (O-H–O) angle lie in the statistically favourable region on the distance-angle plane, defined by PMF ≤ 0 kT. We also reported that a vast majority of hydrogen bonds formed in the ice I_h crystal lie in a smaller sub-region on the PMF landscape, defined by PMF $\leq$ -2 kT [73]. We used these PMF based definitions of hydrogen bonds to compare the tetrahedrally hydrogen bonded fraction of liquid water with the LFTS fractions estimated from other methods. The fraction of tetrahedrally hydrogen bonded water molecules (green dotted lines in Fig. 3) is observed to over-predict the fraction of LFTS environments in liquid water, when compared to the LFTS fractions estimated by other methods. However, it is interesting to note that the fraction of molecules forming four 'ice-like' hydrogen bonds closely follows the trend of tetrahedral liquid fraction estimated by other methods. This suggests that the structural environments indicated by formation of four 'ice-like' hydrogen bonds possibly correlates with the structure of tetrahedral environments in liquid water. But it should be noted that this characterization of a tetrahedral environment based on four ice-like hydrogen bonds can sharply distinguish a molecule to belong to LFTS or not. On the other hand, as explained in the following paragraphs, we can only predict a probability that any given molecule belongs to LFTS based on its θ_{avg} value.

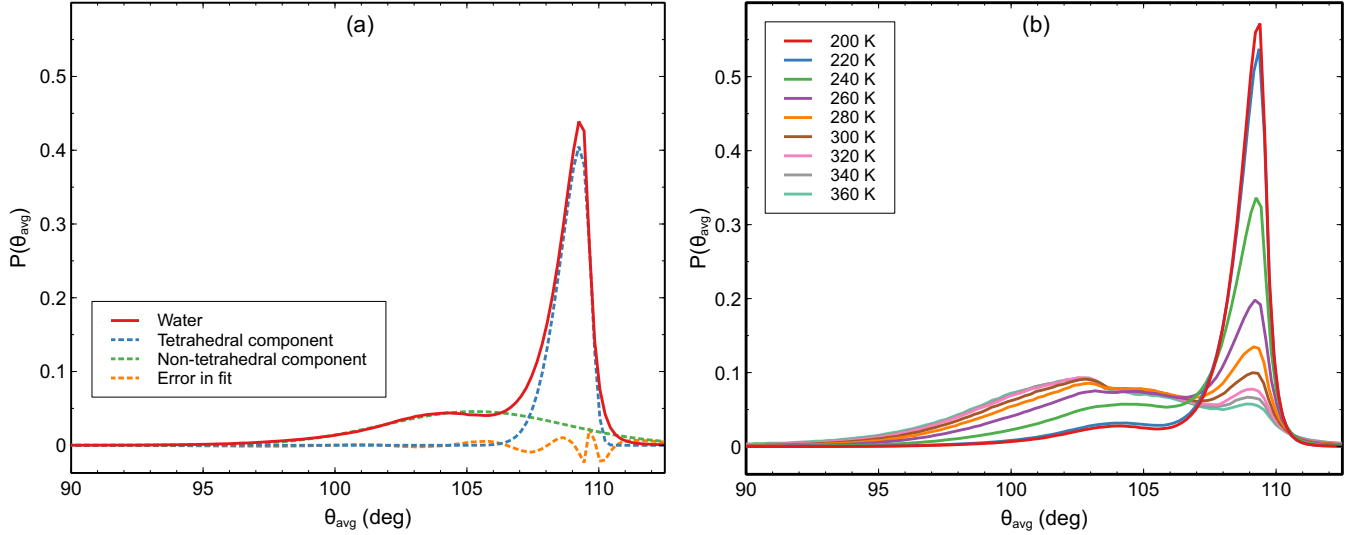Fig. 1a indicates that in the region of lower values

FIG. 1. (a) Decomposing the distribution of the average angles oxygen atoms make with its neighbors (θ_{avg}) to two skewed Gaussian components. The figure demonstrated here corresponds to T= 230 K and P = 1 bar for the iAMOEBA water model. (b) Distribution of average angle an oxygen atom makes with its neighbors (θ_{avg}) at different temperatures and 1 bar. A peak at 109.5° indicates locally tetrahedral environments in liquid water.
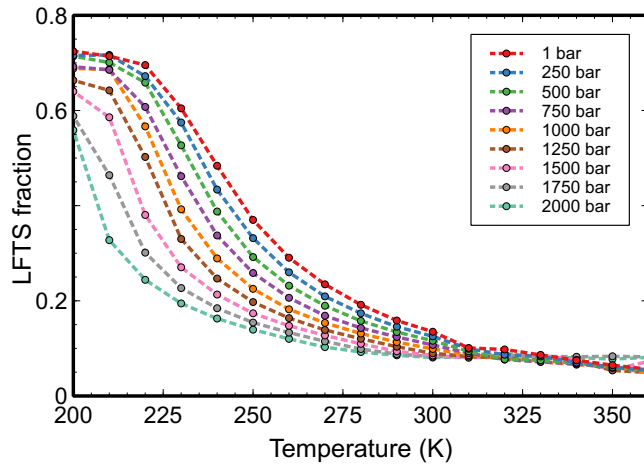

FIG. 2. Fraction of LFTS molecules estimated from the distribution of θ_{avg} values of the iAMOEBA water model.
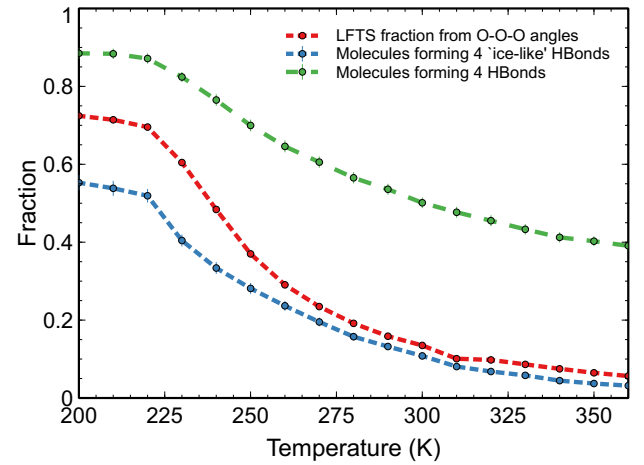

FIG. 3. Fraction of LFTS calculated (P = 1 bar) from O-O-O angles (red) compared to the fraction of molecules forming four 'ice-like' hydrogen bonds (blue), fraction of molecules forming 4 hydrogen bonds (green).

of θ_{avg} ($\theta_{avg} \leq 106°$), the Gaussian component corresponding to tetrahedral structure (blue dotted line in Fig. 1a) is zero, and the entire contribution comes from the non-tetrahedral component (Green dotted line in Fig. 1a). This implies that we can ascertain with full confidence that a water molecule with $\theta_{avg} \leq 106°$ is not a part of tetrahedral environment. However, in the region $106° \leq \theta_{avg} \leq 111°$, Gaussian components corresponding to both tetrahedral and non-tetrahedral components coexist. Therefore, it is difficult to sharply distinguish a given molecule to belong to the tetrahedral form or not when they have values of θ_{avg} in this range. In the region where $106° \leq \theta_{avg} \leq 111°$, where both the Gaussian

components co-exist, molecules can only be classified to belong to LFTS with a finite probability. We use Baye's theorem to calculate the probability with which we can categorise a given molecule to belong to LFTS (equation 5).

$$P(LFTS|\theta_{avg}) =$$
$$\frac{P(\theta_{avg}|LFTS) \times P(LFTS)}{[P(\theta_{avg}|LFTS)P(LFTS)] + [P(\theta_{avg}|LFTS')P(LFTS')]} \quad (5)$$

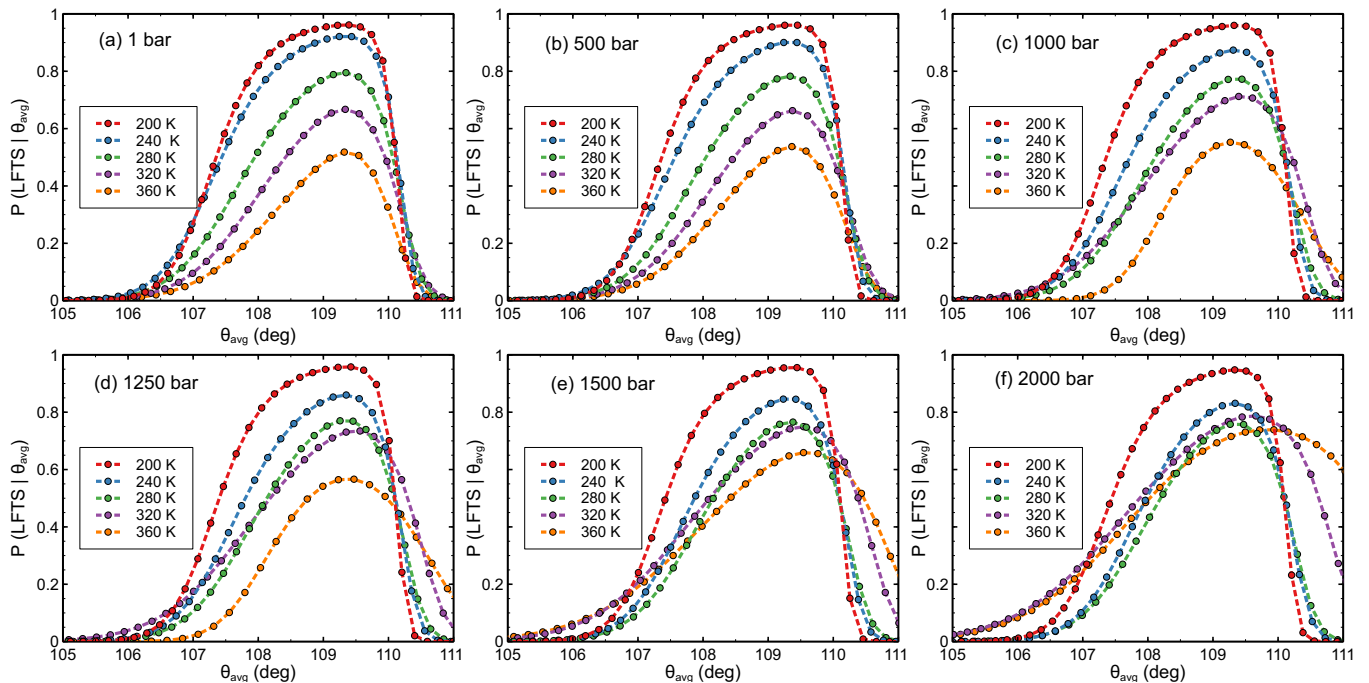where $P(LFTS|\theta_{avg})$ is the probability that a molecule

FIG. 4. The probability of any given molecule belonging to LFTS environment, provided we know its θ_{avg} value. The closer the value of θ_{avg} to 109.5°, the higher the probability that it belongs to LFTS. Also, we find that the certainty of classifying a molecule to LFTS based on its θ_{avg} is higher at lower temperatures.

belongs to LFTS, provided we know its θ_{avg} value. $P(\theta_{avg}|LFTS)$ and $P(\theta_{avg}|LFTS')$ are the probabilities that a molecule with a given value of θ_{avg} is a part of the LFTS or not, respectively. They are essentially the probability densities of the individual Gaussian components corresponding to tetrahedral $(G_{skew}(\theta_{avg}; \mu_s, \sigma_s, \alpha_s))$ and non-tetrahedral $(G_{skew}(\theta_{avg}; \mu_\rho, \sigma_\rho, \alpha_\rho))$ environments respectively, as described in equations 1 and 2. $P(LFTS)$ and $P(LFTS')$ are the estimated fractions of LFTS and non-LFTS molecules. The results are shown in Fig. 4. The two most striking observations from the analysis are (1) the closer the value of θ_{avg} to 109.5°, the higher the certainty with which they can be classified as LFTS, irrespective of the temperature and pressure of the system, (2) there is no value of θ_{avg} for which the probability is 1, indicating that a sharp distinction between LFTS and non-LFTS molecules is not possible.

In general, as the temperature of the system is increased, the probability of belonging to LFTS is lower. This interesting observation indicates that with an increase in temperature, along with the reduction in the fraction of LFTS (as shown in 2a), the magnitude of fluctuations to non-tetrahedral form gets higher, even for molecules with θ_{avg} close to 109.5°. The difference between high-temperature isotherms is more pronounced at lower pressures, indicating that fluctuations into low density environments in liquid water at higher temperatures are less temperature-dependent at higher pressures. On the other hand, at deeply super-cooled temperatures, the differences between the isotherms are more pronounced

at lower pressures.

B. Characterisation of the tetrahedral environment

It is of interest to study the structural characteristics of the LFTS which have been estimated using the methods described in this work. One important order parameter reported in the literature is the Local Structure Index (LSI) [41]. Shiratani and Sasai [41] showed that the distribution of LSI in liquid water can be decomposed to individual distributions corresponding to *structured* and *de-structured* environments. Wikefeldt, Nilsson and Pettersson demonstrated that this parameter is capable of capturing the bi-modality of the *inherent structure* in molecular simulations [40]. LSI is defined by equations 6 and 7.

$$LSI(k,t) = \frac{1}{n(k,t)} \sum_{i=1}^{n(k,t)} \left[\Delta(i:k,t) - \bar{\Delta}(k,t)\right]^2 \quad (6)$$

where,

$$\bar{\Delta}(k,t) = \frac{1}{n(k,t)} \sum_{i=1}^{n(k,t)} \Delta(i;k,t) \quad (7)$$

where $\Delta(i;k,t)$ is $r_{i+1} - r_i$ and r_i is the distance of molecule i from the central molecule k when they are arranged in the ascending order of distances from k. The number of neighbors of molecule k at time t $(n(k,t))$ is

chosen such that $r_{n(k,t)} < 3.7\mathring{A} < r_{n(k,t)+1}$. A higher LSI value indicates a local tetrahedral environment, with the neighbors positioned further from the central molecule, resulting in a low density environment, and a lower LSI value indicates that the neighbors are positioned closer to the central molecule, forming a high density environment.

We compared the distribution of LSI parameters for 4 strongly hydrogen bonded water molecules [73] to the structured component of LSI as reported by Shiratani and Sasai. We find that the distribution of structured component of LSI is similar to the distribution of LSI parameters for four strongly hydrogen bonded water molecules as shown in Fig. 5a. This shows that the structured component of the LSI distribution as described by Shiratani and Sasai [41] points to tetrahedrally hydrogen bonded environments in water. The distribution of LSI of water molecules against the corresponding θ_{avg} in liquid water and ice I$_h$ is shown in Fig. 5b. Ice I$_h$, because of its structure, provides a reference state for the LSI values in a tetrahedral environment. The LSI values of ice I$_h$ crystal ranges from 0 to $\sim$ 0.5, spanning almost entirely through the range of values of liquid water. This is also evident from a huge overlap between the distribution of *structured* and *de-structured* components of LSI reported by Shiratani and Sasai. The distribution of θ_{avg} of ice I$_h$ on the other hand is limited to a narrower range compared to that of the liquid water as seen in Fig. 5b. This enables using θ_{avg} to distinguish tetrahedral environments in the real structure of water. Two distinct clusters are also visible Fig. 5b, one cluster ranging over values similar to θ_{avg} values of ice I$_h$ indicating tetrahedral environment, and another cluster ranging smaller values corresponding to de-structured environment. The cluster at the right (with θ_{avg} around 109.5 °) in Fig. 5b can be observed to have a similar scatter of LSI and θ_{avg} values when compared to ice. This shows that there are water molecules with tetrahedral structure which resemble the structure of ice I$_h$ in liquid water, and validates the assumptions reported by Urbic and Dill [60] in their model of 'cagey water'- like the existence of ice-like structures in liquid water.

To further characterize the structural environments indicated by O-O-O angles, we also report different structural order parameters of molecules against their θ_{avg} values at different temperatures and 1 bar. The number of first shell neighbors, and the average number of hydrogen bonds against the corresponding values of θ_{avg} are shown in Fig. 6a. It is observed that molecules having θ_{avg} values close to 109.5°have almost four neighbors in the first shell. At lower values of θ_{avg} ($90 \leq \theta_{avg}$), molecules have higher number of neighbors in the first shell indicating a denser structural environment. It is also interesting to note that the average number of hydrogen bonds and average number of neighbors approach each other as the value of θ_{avg} is close to 109.5°. This indicates that for a molecule in the tetrahedral environment, the number of neighbors is reduced by forming hydrogen bonds with all (or most) of its neighbors. This indicates the role of hydrogen bond formation in minimising the number of neighbors, when a molecule is a part of a tetrahedral environment. We find that the fraction of molecules forming four hydrogen bonds is maximised in the region where θ_{avg} is close to 109.5°(Fig. 6c). We also find that the number of ice-like hydrogen bonds are maximised for molecules with θ_{avg} close to 109.5°(Fig. 6b). Interestingly, a molecule in a tetrahedral environment does not necessarily form 'ice-like' hydrogen bonds with all of its neighbors. Fig. 6d indicates that the probability of forming four ice-like hydrogen bonds is higher for molecules forming θ_{avg} around 109.5.

We also studied the variation of other structural order parameters that have been used to characterise the tetrahedrality, with θ_{avg} in liquid water. LSI parameter [41] has been used by Wikfeldt et al. [40] to identify spatially inhomogeneous low density environments in liquid water. Wikfeldt et al. [40] categorised molecules based on their LSI values to belong to a high-LSI value class or a low-LSI value class. They observed that the high-LSI species exhibited LDL-like characteristics. The variation of LSI with θ_{avg} at different temperatures is shown in Fig. 6e, and shows that molecules which have θ_{avg} corresponding to tetrahedral order have also high LSI values. This indicates a similarity in the structural environments characterised by high LSI and θ_{avg} close to 109.5°. There is a decline in the LSI values, as temperature is increased. Molecules with same value of θ_{avg} have lower values of LSI at higher temperatures. This is in line with observations by Shi and Tanaka [43] who also suggest that at higher temperatures where the magnitude of thermal fluctuations is severe, LSI is not very efficient in capturing the tetrahedrality of water. On the other hand, θ_{avg} appears to be better in capturing the local tetrahedral environments as indicated by Fig. 6a. The number of neighbors and number of hydrogen bonds remain $\sim$ 4 for molecules with θ_{avg} close to 109.5 °, irrespective of the temperature.

Another order parameter that is used to study ordering in water is the tetrahedral order parameter (q) [74, 75]. This parameter is a widely used [76] orientational order parameter, defined by equation 8.

$$q = 1 - \frac{3}{8}\sum_{j=1}^{3}\sum_{k=j+1}^{4}\left(cos\psi_{jk} + \frac{1}{3}\right)^2 \qquad (8)$$

where ψ_{jk} is the angle formed by a molecule with its jth and kth neighbors. Based on the local structure, this order parameter can assume values from 0 (for an ideal gas) to 1 (for a regular tetrahedron) [75]. A higher value of this order parameter indicates a more tetrahedrally oriented environment. The distribution of the tetrahedral order parameter (q) [74, 75] against θ_{avg} was also studied (Fig. 6f). We observe that molecules in tetrahedral environments as indicated by the θ_{avg} parameter have highest values of tetrahedral order parameter, at all
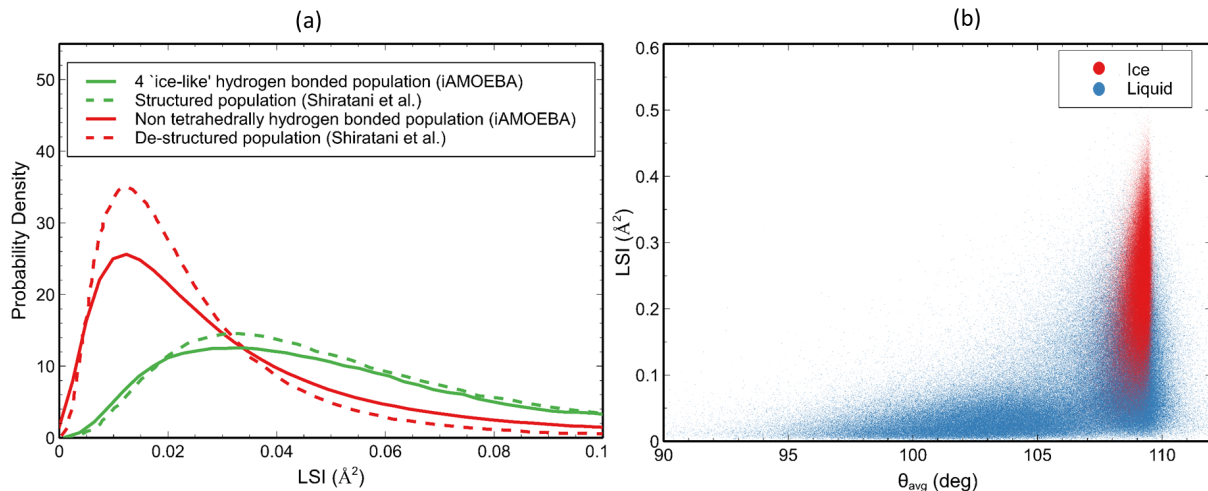
FIG. 5. (a) Distribution of LSI of structured (green dotted) and de-structured (red dotted) environments in water reported by Shiratani and Sasai [41] compared with distribution of LSI values of water molecules forming 4 'ice-like' hydrogen bonds (green continuous) and other molecules (red continuous), calculated using the iAMOEBA water model (T= 300 K, P= 1 bar). The 'ice-like' structures are calculated based on the definition by us [73]. (b) Scatter plot of LSI values and average angle oxygen atom forms with its neighbors (θ_{avg}) in liquid water (blue dots) and ice I$_h$ (red dots), from simulations of iAMOEBA water at 230 K and 1 bar.

temperatures. As described previously, ψ_{jk} mentioned in equation 8 is the O-O-O angle made by a given molecule with its jth and kth neighbors, and therefore, molecules having θ_{avg} close to 109.5°exhibiting high value of q can be expected, as is shown in Fig. 6f. The temperature dependency of q can also be seen from Fig. 6f. As the temperature is increased, it is observed that the value of q is lower. Even for molecules with θ_{avg} close to 109.5°, the value of q is observed to be lower at higher temperatures, indicating fluctuations into non-tetrahedral environments. This observation also indicates the effect of thermal fluctuations on the capability of tetrahedral order parameter (q) in characterizing the structural forms of water, as suggested by Shi and Tanaka [43].

Even though the methods described here have been demonstrated to be useful in characterizing the two structural forms underlying LLPT in water, commenting on the nature of the phase transition requires further analysis. The time scale over which phase-transition is reported to happen [39] is much longer than the lengths of the simulations we have analysed. However, since the method can characterise the underlying structure of the different local environments, it may be potentially used in a future work to explore the nature of phase transition.

IV. CONCLUSIONS

We use the angles that an oxygen atom makes with its neighbors to characterise the structural environments in liquid water. Instead of using the distribution of *all angles* an oxygen atom makes with its neighbors, we use the *average angle* (θ_{avg}) it makes with its neighbors, be-

cause it is more beneficial in characterising the low density environments in water. The distribution of θ_{avg} has two peaks- one close to 109.5°- corresponding to low density tetrahedral environments and one at lower angles - corresponding to non-tetrahedral high density environments. We observe that the magnitude of the peak at 109.5°decreases when the temperature of the system is increased, indicating a decline in the tetrahedral form in water. The distribution is decomposed into two constituent skewed Gaussian components,- one corresponding to each structural form in water. By decomposing the distribution of θ_{avg} into two constituent components, we estimate the fraction of LFTS environments in water over a wide range of temperatures and pressures, and try to gain insights into the structure of low density environments in water. We find a qualitative similarity between the LFTS fractions reported in this work and the trends in literature [6].

An important question that we tried to address is the physical boundary of the two structural forms. The constituent components of the distribution are found to overlap, there-by suggesting that a sharp distinction between the two structural forms is not possible using θ_{avg}. This means that we cannot identify sharp physical boundaries separating the two structural forms using θ_{avg}. However, we quantified the certainty with which we may say if a given molecule belongs to LFTS, provided we know the average angle it makes with its neighboring molecules.

We also studied the structural properties of tetrahedral liquid water, and find that the tetrahedral environments identified by our method has similarities with structural environments that are described by other order parameters like the LSI, number of first shell neighbors, number
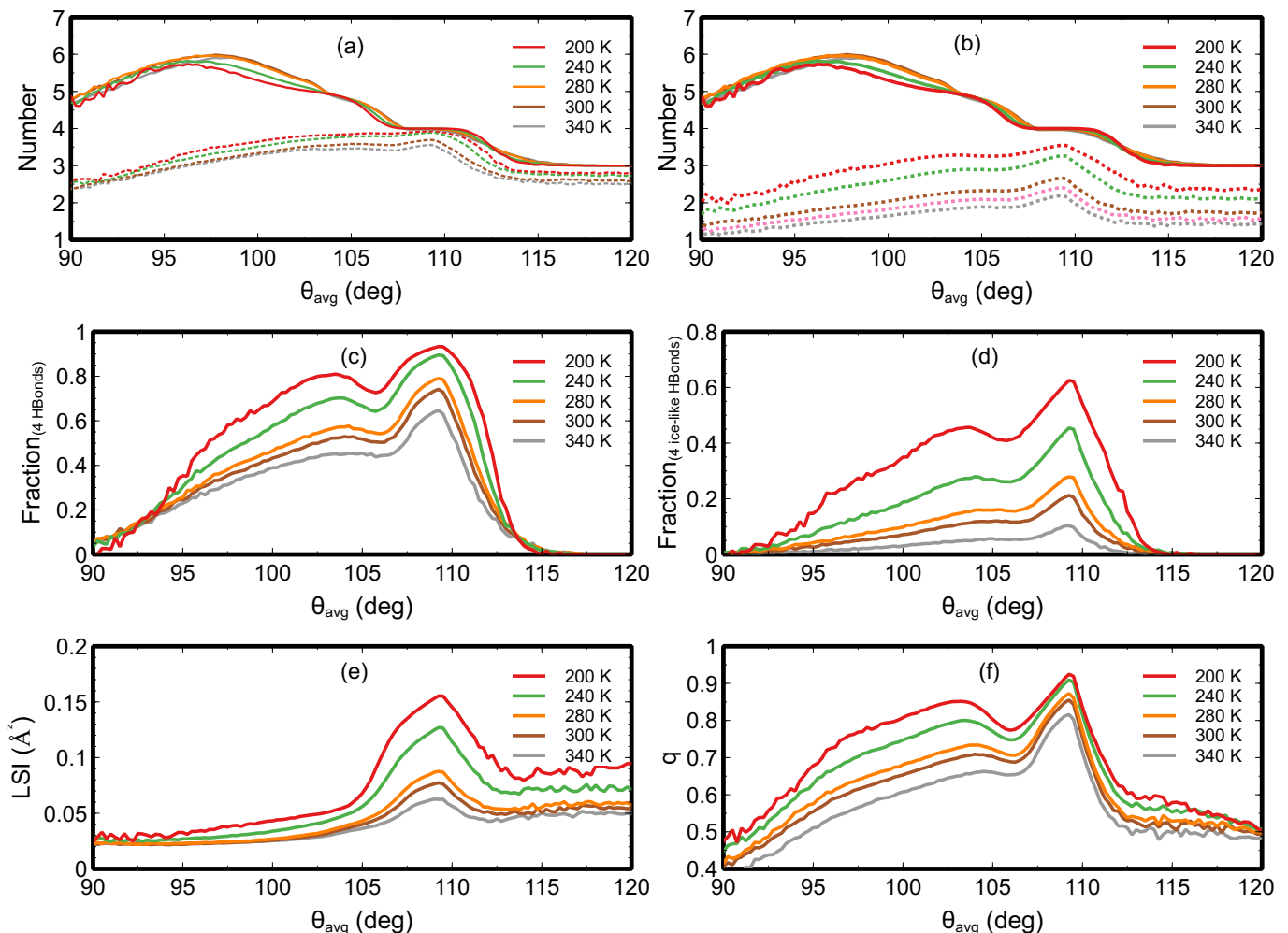
FIG. 6. Characterisation of tetrahedral environments indicated by θ_{avg} at various temperatures and 1 bar. The average property of water molecules is plotted on the y-axis against its corresponding θ_{avg}. (a) Comparison of number of first shell neighbors, and number of hydrogen bonds, (b) comparison of number of first shell neighbors and the number of ice-like hydrogen bonds (c) fraction of molecules forming four hydrogen bonds. (d) fraction of molecules forming four ice-like hydrogen bonds (e) LSI order parameter and (f) tetrahedral order parameter (q).

of hydrogen bonds and tetrahedral order parameter (q). We find that the molecules with θ_{avg} close to 109.5°, are the molecules that have high LSI and q values. The tetrahedral liquid identified by θ_{avg} is also found to minimise the number of their first shell neighbors and forms hydrogen bonds with almost all of their neighbors. An intersting observation is that the fraction of LFTS molecules identified using this method is very similar to the fraction of molecules forming 4 'ice-like' hydrogen bonds in water. The results of our study introduce a new parameter to identify low density liquid fraction in water, and indicate the similarities between different order parameters that have been reported in literature. The analysis also gives insights into the role of hydrogen bond formation in forming low density liquid environments in water. By extending the methods proposed by us to characterise the two structural forms in water, it may also be able to

characterise the nature of phase transition between the two structural forms.

[1] H. Tanaka, J. Chem. Phys. **112**, 799 (2000).
[2] H. Tanaka, Physical Review E **62**, 6968 (2000).
[3] H. Tanaka, Phys. Rev. B **66**, 064202 (2002).
[4] H. Tanaka, Eur. Phys. J. E **35**, 1 (2012).
[5] L. G. M. Pettersson, Int. Conf. Phys. Liq. Matter: Modern Problems , 3 (2018).
[6] J. Russo and H. Tanaka, Nat. Commun. **5**, 1 (2014).
[7] H. Whiting, Proc. Am. Acad. Arts Sci. **19**, 353 (1883).
[8] W. C. Röntgen, Ann. Phys. **281**, 91 (1892).
[9] C. Davis Jr and T. Litovitz, J. Chem. Phys. **42**, 2563 (1965).
[10] C. A. Angell, J. Phys. Chem. **75**, 3698 (1971).
[11] M. Vedamuthu, S. Singh, and G. W. Robinson, J. Phys. Chem. **98**, 2222 (1994).
[12] P. Gallo, K. Amann-Winkel, C. A. Angell, M. A. Anisimov, F. Caupin, C. Chakravarty, E. Lascaris, T. Loerting, A. Z. Panagiotopoulos, J. Russo, and et al, Chem. Rev. **116**, 7463 (2016).
[13] V. Holten and M. Anisimov, Sci. Rep. **2**, 1 (2012).
[14] R. Shi, J. Russo, and H. Tanaka, J. Chem. Phys. **149**, 224502 (2018).
[15] O. Mishima, J. Chem. Phys. **133**, 144503 (2010).
[16] L. Xu, P. Kumar, S. V. Buldyrev, S.-H. Chen, P. H. Poole, F. Sciortino, and H. E. Stanley, Proc. Natl. Acad. Sci. U.S.A. **102**, 16558 (2005).
[17] D. Fuentevilla and M. Anisimov, Phys. Rev. Lett. **97**, 195702 (2006).
[18] D. Fuentevilla and M. Anisimov, Phys. Rev. Lett. **98**, 149904 (2007).
[19] C. Bertrand and M. Anisimov, J. Phys. Chem. B **115**, 14099 (2011).
[20] P. H. Poole, F. Sciortino, U. Essmann, and H. E. Stanley, Nature **360**, 324 (1992).
[21] O. Mishima and H. E. Stanley, Nature **396**, 329 (1998).
[22] H. Stanley, P. Kumar, G. Franzese, L. Xu, Z. Yan, M. G. Mazza, S. Buldyrev, S.-H. Chen, and F. Mallamace, Eur. Phys. J.: Spec. Top. **161**, 1 (2008).
[23] D. T. Limmer and D. Chandler, J. Chem. Phys. **135**, 134503 (2011).
[24] D. T. Limmer and D. Chandler, J. Chem. Phys. **138**, 214504 (2013).
[25] D. Chandler, Nature **531**, E1 (2016).
[26] A. Nilsson, C. Huang, and L. G. Pettersson, J. Mol. Liq. **176**, 2 (2012).
[27] A. Nilsson and L. G. Pettersson, Nat. Commun. **6**, 1 (2015).
[28] F. Perakis, K. Amann-Winkel, F. Lehmkühler, M. Sprung, D. Mariedahl, J. A. Sellberg, H. Pathak, A. Späh, F. Cavalca, D. Schlesinger, et al., Proc. Natl. Acad. Sci. U.S.A. **114**, 8193 (2017).
[29] K. H. Kim, A. Späh, H. Pathak, F. Perakis, D. Mariedahl, K. Amann-Winkel, J. A. Sellberg, J. H. Lee, S. Kim, J. Park, et al., Science **358**, 1589 (2017).
[30] K. H. Kim, K. Amann-Winkel, N. Giovambattista, A. Späh, F. Perakis, H. Pathak, M. L. Parada, C. Yang, D. Mariedahl, T. Eklund, et al., Science **370**, 978 (2020).
[31] O. Mishima, L. Calvert, and E. Whalley, Nature **314**, 76 (1985).
[32] T. Loerting, V. Fuentes-Landete, P. H. Handle, M. Seidl, K. Amann-Winkel, C. Gainaru, and R. Böhmer, J. Non-Cryst. Solids **407**, 423 (2015).
[33] N. Giovambattista, T. Loerting, B. R. Lukanov, and F. W. Starr, Sci. Rep. **2**, 1 (2012).
[34] R. J. Speedy, J. Phys. Chem. **86**, 982 (1982).
[35] J. C. Palmer, R. Car, and P. G. Debenedetti, Faraday Discuss. **167**, 77 (2013).
[36] J. C. Palmer, F. Martelli, Y. Liu, R. Car, A. Z. Panagiotopoulos, and P. G. Debenedetti, Nature **531**, E2 (2016).
[37] J. C. Palmer, A. Haji-Akbari, R. S. Singh, F. Martelli, R. Car, A. Z. Panagiotopoulos, and P. G. Debenedetti, J. Chem. Phys. **148**, 137101 (2018).
[38] J. C. Palmer, P. H. Poole, F. Sciortino, and P. G. Debenedetti, Chem. Rev. **118**, 9129 (2018).
[39] P. G. Debenedetti, F. Sciortino, and G. H. Zerze, Science **369**, 289 (2020).
[40] K. Wikfeldt, A. Nilsson, and L. G. Pettersson, Phys. Chem. Chem. Phys. **13**, 19918 (2011).
[41] E. Shiratani and M. Sasai, J. Chem. Phys. **104**, 7671 (1996).
[42] P. G. Debenedetti and F. H. Stillinger, Nature **410**, 259 (2001).
[43] R. Shi and H. Tanaka, The Journal of chemical physics **148**, 124503 (2018).
[44] N. Ansari, R. Dandekar, S. Caravati, G. Sosso, and A. Hassanali, J. Chem. Phys. **149**, 204507 (2018).
[45] M. G. Alinchenko, A. V. Anikeenko, N. N. Medvedev, V. P. Voloshin, M. Mezei, and P. Jedlovszky, J. Phys. Chem. B **108**, 19056 (2004).
[46] N. N. Medvedev, V. Voloshin, V. Luchnikov, and M. L. Gavrilova, J. Comput. Chem. **27**, 1676 (2006).
[47] R. Shi and H. Tanaka, Journal of the American Chemical Society **142**, 2868 (2020).
[48] S. Kumari, A. V. Muthachikavil, J. K. Tiwari, and S. N. Punnathanam, Langmuir **36**, 2439 (2020).
[49] S. Chakraborty and B. Jana, Phys. Chem. Chem. Phys. **21**, 19298 (2019).
[50] S. Parui and B. Jana, J. Phys. Chem. B **121**, 7016 (2017).
[51] S. Parui and B. Jana, J. Phys. Chem. B **122**, 9827 (2018).
[52] B. Jana, R. S. Singh, R. Biswas, and B. Bagchi, Current Science , 900 (2011).
[53] L. Zheng, M. Chen, Z. Sun, H.-Y. Ko, B. Santra, P. Dhuvad, and X. Wu, J. Chem. Phys. **148**, 164505 (2018).
[54] R. A. DiStasio Jr, B. Santra, Z. Li, X. Wu, and R. Car, J. Chem. Phys. **141**, 084502 (2014).
[55] A. K. Soper and M. A. Ricci, Phys. Rev. Lett. **84**, 2881 (2000).
[56] P. A. Giguère, J. Raman Spectrosc. **15**, 354 (1984).
[57] M. Chen, H.-Y. Ko, R. C. Remsing, M. F. C. Andrade, B. Santra, Z. Sun, A. Selloni, R. Car, M. L. Klein, J. P. Perdew, et al., Proc. Natl. Acad. Sci. U.S.A. **114**, 10846 (2017).
[58] R. Shi and H. Tanaka, Proc. Natl. Acad. Sci. U.S.A. **117**, 26591 (2020).
[59] H. Pathak, J. Palmer, D. Schlesinger, K. T. Wikfeldt, J. A. Sellberg, L. G. Pettersson, and A. Nilsson, J. Chem. Phys. **145**, 134507 (2016).
[60] T. Urbic and K. A. Dill, Journal of the American Chemical Society **140**, 17106 (2018).
[61] L.-P. Wang, T. Head-Gordon, J. W. Ponder, P. Ren, J. D. Chodera, P. K. Eastman, T. J. Martinez, and V. S. Pande, J. Phys. Chem. B **117**, 9956 (2013).

[62] G. A. Cisneros, K. T. Wikfeldt, L. Ojamae, J. Lu, Y. Xu, H. Torabifard, A. P. Bartok, G. Csanyi, V. Molinero, and F. Paesani, Chem. Rev. **116**, 7501 (2016).

[63] O. Demerdash, E.-H. Yap, and T. Head-Gordon, Annu. Rev. Phys. Chem. **65**, 149 (2014).

[64] I. Shvab and R. J. Sadus, Fluid Phase Equilib. **407**, 7 (2016).

[65] P. Eastman, J. Swails, J. D. Chodera, R. T. McGibbon, Y. Zhao, K. A. Beauchamp, L.-P. Wang, A. C. Simmonett, M. P. Harrigan, C. D. Stern, et al., PLoS Comput. Biol. **13**, e1005659 (2017).

[66] J. A. Izaguirre, C. R. Sweet, and V. S. Pande, in Biocomputing 2010 (World Scientific, 2010) pp. 240–251.

[67] K.-H. Chow and D. M. Ferguson, Comput. Phys. Commun. **91**, 283 (1995).

[68] J. Åqvist, P. Wennerström, M. Nervall, S. Bjelic, and B. O. Brandsdal, Chem. Phys. Lett. **384**, 288 (2004).

[69] R. J. Gowers, M. Linke, J. Barnoud, T. J. E. Reddy, M. N. Melo, S. L. Seyler, J. Domanski, D. L. Dotson, S. Buchoux, I. M. Kenney, et al., Los Alamos National Lab.(LANL), Los Alamos, NM (United States) (2019).

[70] R. D. Fraser and E. Suzuki, Analytical chemistry **41**, 37 (1969).

[71] See Supplemental Material at [] for a discussion on the use of all O-O-O angles, demonstration of the methods using TIP4P/2005 water model, and the estimated values of the model parameters.

[72] J. W. Biddle, V. Holten, and M. A. Anisimov, J. Chem. Phys. **141**, 074504 (2014).

[73] A. V. Muthachikavil, B. Peng, G. M. Kontogeorgis, and X. Liang, J. Phys. Chem. B **125**, 7187 (2021).

[74] P.-L. Chau and A. Hardwick, Molecular Physics **93**, 511 (1998).

[75] J. R. Errington and P. G. Debenedetti, Nature **409**, 318 (2001).

[76] E. Duboué-Dijon and D. Laage, J. Phys. Chem. B **119**, 8406 (2015).

[77] J. L. Abascal and C. Vega, J. Chem. Phys. **123**, 234505 (2005).

[78] C. Vega and J. L. Abascal, Phys. Chem. Chem. Phys. **13**, 19663 (2011).

[79] J. L. Abascal and C. Vega, The Journal of Chemical Physics **133**, 234502 (2010).

[80] A. Späh, H. Pathak, K. H. Kim, F. Perakis, D. Mariedahl, K. Amann-Winkel, J. A. Sellberg, J. H. Lee, S. Kim, J. Park, et al., Phys. Chem. Chem. Phys. **21**, 26 (2019).

[81] R. W. Hockney, S. Goel, and J. Eastwood, J. Comput. Phys. **14**, 148 (1974).

[82] S. Nosé, Mol. Phys. **52**, 255 (1984).

[83] W. G. Hoover, Phys. Rev. A **31**, 1695 (1985).

[84] S. Nosé, J. Chem. Phys. **81**, 511 (1984).

[85] M. Parrinello and A. Rahman, Phys. Rev. Lett. **45**, 1196 (1980).

[86] M. Parrinello and A. Rahman, J. Appl. Phys. **52**, 7182 (1981).

[87] D. Van Der Spoel, E. Lindahl, B. Hess, G. Groenhof, A. E. Mark, and H. J. Berendsen, J. Comput. Chem. **26**, 1701 (2005).